01 Jan 2005

A Heuristic-Dynamic-programming-Based Power System Stabilizer for a Turbogenerator in a Single-Machine Power System

Wenxin Liu

Ganesh K. Venayagamoorthy
Missouri University of Science and Technology

Donald C. Wunsch
Missouri University of Science and Technology, dwunsch@mst.edu

Recommended Citation

A Heuristic-Dynamic-Programming-Based Power System Stabilizer for a Turbogenerator in a Single-Machine Power System

Wenxin Liu, *Student Member, IEEE*, Ganesh Kumar Venayagamoorthy, *Senior Member, IEEE*, and Donald C. Wunsch, II, *Fellow, IEEE*

Abstract—Power system stabilizers (PSSs) are used to generate supplementary control signals for the excitation system in order to damp the low-frequency power system oscillations. To overcome the drawbacks of a conventional PSS (CPSS), numerous techniques have been proposed in the literature. Based on the analysis of existing techniques, a novel design based on heuristic dynamic programming (HDP) is presented in this paper. HDP, combining the concepts of dynamic programming and reinforcement learning, is used in the design of a nonlinear optimal power system stabilizer. Results show the effectiveness of this new technique. The performance of the HDP-based PSS is compared with the CPSS and the indirect-adaptive-neurocontrol-based PSS under small and large disturbances. In addition, the impact of different discount factors in the HDP PSS's performance is presented.

Index Terms—Adaptive critic design (ACD), discount factors, heuristic dynamic programming (HDP), indirect adaptive control, neural networks, neuro-control, neuro-identifier, online training, power system stabilizer (PSS).

I. INTRODUCTION

CURRENTLY, most generators are equipped with voltage regulators to automatically control the terminal voltage. It is known that the voltage regulator action had a detrimental impact upon the dynamic stability of the power system. Oscillations of small magnitude and low frequency often persist for a long time and in some cases even present limitations on power transfer capability [1].

In the analysis and control of power system stability, two distinct modes of system oscillations are usually recognized. One mode is associated with generators at a generating station swinging with respect to the rest of the power system. Such oscillations are referred to as "intra-area" oscillations. The second mode oscillation is associated with the swinging of many machines in the one area of the system against machines in other areas. This is referred to as "inter-area" oscillations.

Power system stabilizers (PSSs) are used to generate supplementary control signals for the excitation system in order to damp both types of oscillations.

Conventional power system stabilizers (CPSSs) are designed using the theory of phase compensation in the frequency domain and are introduced as a lead–lag compensator. The parameters of CPSS are determined based on a linearized model of the power system. To have the CPSS provide good damping over a wide operating range, its parameters need to be fine tuned in response to both modes of oscillations. Since power systems are highly nonlinear systems, with configurations and parameters that change with time, the CPSS design based on a linearized model of the power system cannot guarantee its performance in a practical operating environment. Thus, an adaptive PSS which caters for the nonlinear nature of the plant by adapting its parameters to the changes in the environment is required for the power system.

To improve the performance of CPSSs, numerous techniques have been proposed for their design, such as using intelligent optimization methods (simulated annealing, genetic algorithm, tabu search) [2]–[4], fuzzy logic [5], [6], neural networks, and many other nonlinear control techniques [7]–[9]. The intelligent optimization algorithms are used to determine the optimal parameters for CPSS by optimizing an eigenvalue based cost function in an offline mode. Since the method is based on a linearized model and the parameters are not updated online, they lack satisfactory performance during practical operation. The rule-based fuzzy logic control methods are well known for the difficulty in obtaining and adjusting the parameters of the rules, especially online. Recently, more emphasis has been placed on the combined usage of fuzzy systems and other technologies such as neural networks to add adaptability to the design [10]. Currently, most of the nonlinear control based methods use simplified models to decrease complexity of the algorithms. Considering the complexity of practical power systems, a more realistic model with less computation time is required for effective robust control over a wide range of operating conditions.

Since neural networks have the advantages of high computation speed, generalization, and learning ability, they have been successfully applied to the identification and control of nonlinear systems. The work on the application of neural networks to the PSS design so far includes online tuning of CPSS parameters [11], [12], the implementation of inverse model control [13], [14], direct control [15], and indirect adaptive control [16]–[21]. The online tuning of CPSS parameters
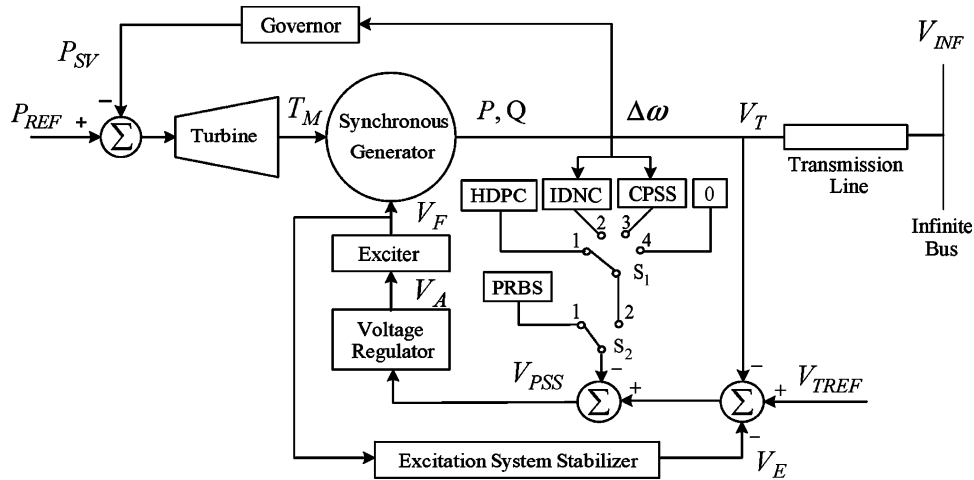
Fig. 1.   System model configuration.

and the inverse model control do not update the weights of neural networks online, so their performances highly depend on the quality of offline training samples, which are difficult to obtain. The indirect adaptive neurocontrol design consists of two neural networks, namely, the neuro-controller and the neuro-identifier. The neuro-controller is used to generate the stabilizing supplementary control signal to the plant and the neuro-identifier is used to provide a dynamic model of the plant to evaluate and update the weights of the neuro-controller. Since the plant model is not used in the direct adaptive neural network control structure, computation time is decreased. However, there is no accurate way to directly evaluate the performance of the controller, especially when the system parameters are changing over time; therefore, this is not the most effective control technique, especially for power systems.

The risk with the indirect adaptive neurocontrol scheme is that the training of the controller is carried out all the time, which can lead to instability under large disturbances and unknown uncertainties. In this paper, a novel heuristic-dynamic-programming (HDP)-based optimal power system stabilizer is proposed. HDP is a class of adaptive critic designs which provides optimal control. With adaptive critic designs, neural networks with fixed weights are used as tools for implementing optimal controllers which is a potential benefit in overcoming stability issues. The proposed HDP based PSS is evaluated on a single machine infinite bus power system against those of CPSS and indirect adaptive neurocontrol designs. Simulation results are provided to show the performances of the different controllers. In addition, the impact of the choice of discount factors on the HDP PSS's performance is presented.

The power system model is described in Section II. The introduction to HDP and the design of the HDP-based PSS are described in Section III. The training process of the HDP PSS is described in Section IV. Some simulation results are provided in Section IV. Section V concludes the paper.

II. POWER SYSTEM MODEL

The single-machine infinite bus power system (SMIB) model used to evaluate the indirect-neural-network-control-based controller (IDNC) is shown in Fig. 1. The SMIB called the *plant* in

this paper consists of a synchronous generator, a turbine, a governor, an excitation system, and a transmission line connected to an infinite bus. The model is built in MATLAB /SIMULINK environment using the Power System Blockset [22]. In Fig. 1, P_{REF} is the mechanical power reference, P_{SV} is the feedback through the governor, T_M is the turbine output torque, V_{INF} is the infinite bus voltage, V_{TREF} is terminal voltage reference, V_T is terminal voltage, V_A is the voltage regulator output, V_F is field voltage, V_E is the excitation system stabilizing signal, $\Delta\omega$ is the speed deviation, V_{PSS} is the PSS output signal, P is the active power, and Q is the reactive power at the generator terminal.

In Fig. 1, the switch S_1 is used to carry out tests on the power system with HDP-based controller (HDPC), IDNC, and CPSS and without PSS (with switch S_1 at position 1, 2, 3, and 4 respectively). Switch S_2 is used to select between normal operation and training phase (positions 1 and 2, respectively).

The synchronous generator is described by a seventh-order d–q-axes set of equations with the machine current, speed, and rotor angle as the state variables. The turbine is used to drive the generator and the governor is used to control the speed and the real power. The block diagram of the turbine and the conventional governor are shown in Fig. 2.

The excitation system for the generator is modeled according to IEEE Std. 421.5 [23]. The block diagram of the excitation system is shown in Fig. 3.

The CPSS consists of two phase-lead compensation blocks, a signal washout block, and a gain block. The input signal is the rotor speed deviation $\Delta\omega$ [24]. The block diagram of the CPSS is shown in Fig. 4.

The parameters for the generator, automatic voltage regulator (AVR), excitation system, turbine, and governor are given in the Appendix [23]–[25].

III. HDP-BASED PSS DESIGN

A. Background

Adaptive critic designs (ACDs) are neurocontrollers capable of optimization over time, under conditions of noise and uncertainty. A family of ACDs was proposed by Werbos [26] as an
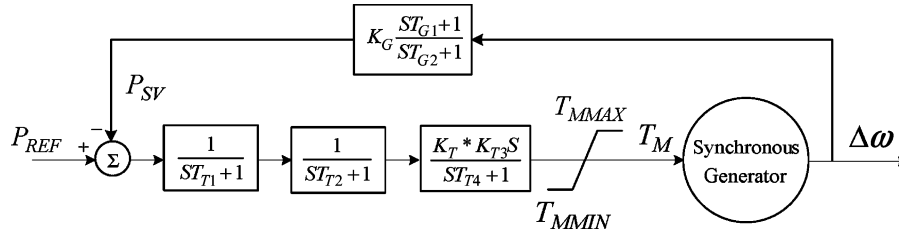
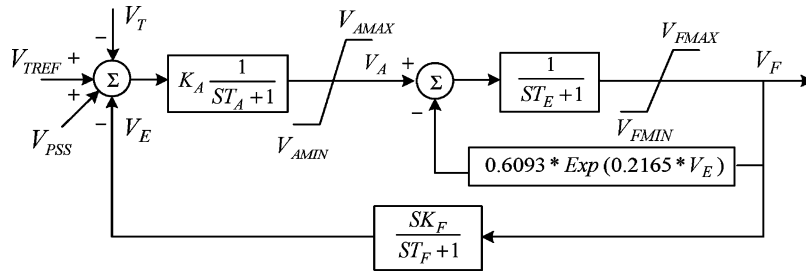Fig. 2.   Block diagram of the turbine and the governor.

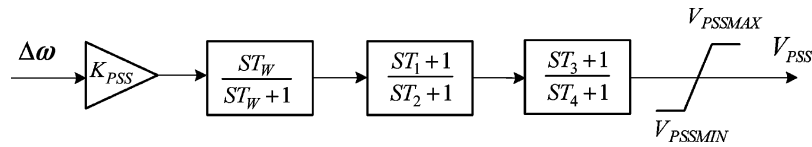Fig. 3.   Block diagram of the excitation system.

Fig. 4.   Block diagram of the conventional power system stabilizer.

optimization technique combining the concepts of reinforcement learning and approximate dynamic programming. For a given series of control actions that must be taken sequentially, and not knowing the effect of these actions until the end of the sequence, it is possible to design an optimal controller using the traditional supervised learning neural network.

The adaptive critic method determines optimal control laws for a system by successively adapting two artificial neural networks (ANNs), namely, an action neural network (which dispenses the control signals) and a critic network (which learns the desired performance index for some function associated with the performance index). These two neural networks approximate the Hamilton–Jacobi–Bellman equation associated with optimal control theory. The adaptation process starts with a nonoptimal, arbitrarily chosen control by the action network; the critic network then guides the action network toward the optimal solution at each successive adaptation. During the adaptations, neither of the networks needs any "information" of an optimal trajectory, only the desired cost needs to be known. Furthermore, this method determines optimal control policy for the entire range of initial conditions and needs no external training, unlike other neurocontrollers [27].

The design ladder of ACDs includes three basic implementations: HDP, Dual Heuristic Programming (DHP), and Globalized Dual Heuristic Programming (GDHP), in the order of increasing power and complexity. The interrelationships between members of the ACD family have been generalized and explained in [28]. In this paper, the simple and powerful HDP approach is adopted for the design of a power system stabilizer.
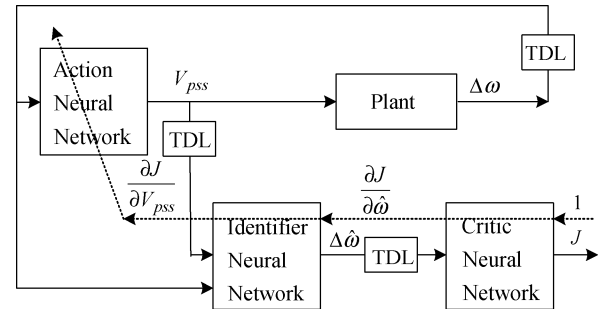

Fig. 5.   General structure of the HDP-based PSS design (dashed lines show backpropagation paths).

B. General Control Structure

The HDP PSS consists of three neural networks, which are: the action, the identifier, and the critic networks. The action network is used to generate the stabilizing supplementary control signals; the identifier network is used to model the plant and estimate its output; the critic network is used to estimate *cost-to-go* function J given by the Bellman's equation. The general structure of the HDPC is shown in Fig. 5.

To simply the description of the training process, it is necessary to clarify the time-step definitions. Both $V_{\text{pss}}(k)$ and $\Delta\omega(k)$ signals are sampled at time step k, but $\Delta\omega(k)$ is not the response for the control signal $V_{\text{pss}}(k)$. Due to the time lag property of the plant, the impact of the control signal $V_{\text{pss}}(k)$ is reflected in the next time sample of the output signal $\Delta\omega(k+1)$. The following sections describe the designs of the three neural networks.
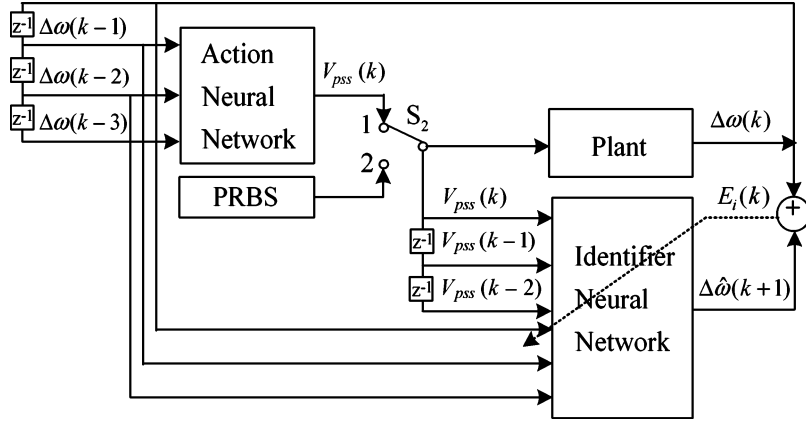
Fig. 6. Training of the neuro-identifier during pre-control (dashed line shows backpropagation pathway).

C. Identifier Neural Network Design

The identifier neural network is developed using the series-parallel Nonlinear Auto Regressive Moving Average (NARMA) model [29]. The model output $\hat{y}$ at time $k + 1$ depends on both past n values of output and m past values of input. The neuro-identifier output equation takes the form given by (1)

$$\hat{y}(k+1) = f\left[\begin{array}{l} y(k), y(k-1), \ldots, y(k-n+1) \\ u(k), u(k-1), \ldots, u(k-m+1) \end{array}\right] \quad (1)$$

where $y(k)$ and $u(k)$ represent the output and input of the plant to be controlled at time k. For this particular system, y, u, and $\hat{y}$ are the speed deviation $\Delta\omega$ of the plant, the output of the action network V_{pss}, and the estimated plant output $\Delta\hat{\omega}(k)$ by the identifier network respectively. Here, both m and n are chosen to be two. One reason for choosing three time-step values is because a third order model of the system is sufficient for the study of transient stability. The other reason is that more time delays means more computation and one author's previous work verified that three time delays is enough for this kind of problem [25].

The identifier network is a multilayer feedforward network trained with the standard backpropagation (BP) algorithm. The numbers of neurons in the input, hidden and output layers are determined empirically and are six, ten, and one, respectively. Considering the ranges of $\Delta\omega$ and V_{pss}, scaling factors of 400 and 2 are used for $\Delta\omega$ and V_{pss}, respectively, to speed up the training process.

The training process of the identifier network is shown in Fig. 6. The inputs to the identifier network are $[\Delta\omega(k-1), \Delta\omega(k-2), \Delta\omega(k-3), V_{\text{pss}}(k-1), V_{\text{pss}}(k-2), V_{\text{pss}}(k-3)]$ and its output is $\Delta\hat{\omega}(k)$. The desired output is the output of the plant $\Delta\omega(k)$. The cost function for training the identifier network is given by (2)

$$J_i(k) = \frac{1}{2}e_i(k)^2 = \frac{1}{2}\left[\Delta\omega(k) - \Delta\hat{\omega}(k)\right]^2. \quad (2)$$

During pre-training of the identifier, the switch S_2 is at position 2 so that a Pseudo Random Binary Signal (PRBS) of small magnitude is used to replace the action network output in order to excite all possible dynamics of the plant [21]. During the post-training, the switch S_2 is at position 1 so that the actual
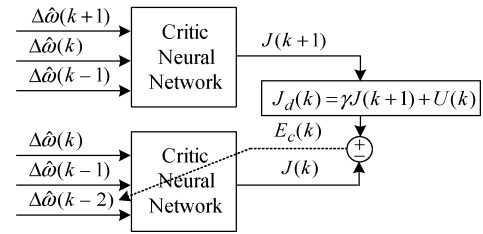

Fig. 7. Training process of the critic network (dashed line shows backpropagation path).

control signal calculated by the action network can be fed to both the plant and the identifier [25].

D. Critic Neural Network Design

The critic network is also a multilayer feedforward network trained with the BP algorithm. The numbers of neurons in the input, hidden and output layers are chosen empirically to be three, six, and one, respectively. The inputs to the critic network are the estimated speed deviation $\Delta\hat{\omega}$ (output of the identifier network) and its two previous values and the output of the critic network is the estimated *cost-to-go* function J, which is defined as

$$J(k) = \sum_{i=0}^{\infty} \gamma^i U(k+i) \quad (3)$$

where γ is the discount factor for finite horizon problems with the range of [0, 1] and is chosen to be 0.5 in this design. $U(k)$ is the utility function or the local cost function. Due to the inertia of the plant, the local/immediate cost $U(k)$ at every time step is dependent on the present and past speed deviations [25] and is given by

$$U(k) = [0.4\Delta\hat{\omega}(k) + 0.4\Delta\hat{\omega}(k-1) + 0.16\Delta\hat{\omega}(k-2)]^2. \quad (4)$$

The training process of the critic network is illustrated in Fig. 7. During training, first the critic network is fed with the outputs of the identifier network at three time instants $[\Delta\hat{\omega}(k), \Delta\hat{\omega}(k-1), \Delta\hat{\omega}(k-2)]$, to calculate the estimated cost-to-go function $J(k)$. Then, the critic network is fed with $[\Delta\hat{\omega}(k+1), \Delta\hat{\omega}(k), \Delta\hat{\omega}(k-1)]$ to calculate the estimated cost-to-go function $J(k+1)$. According to the Bellman's
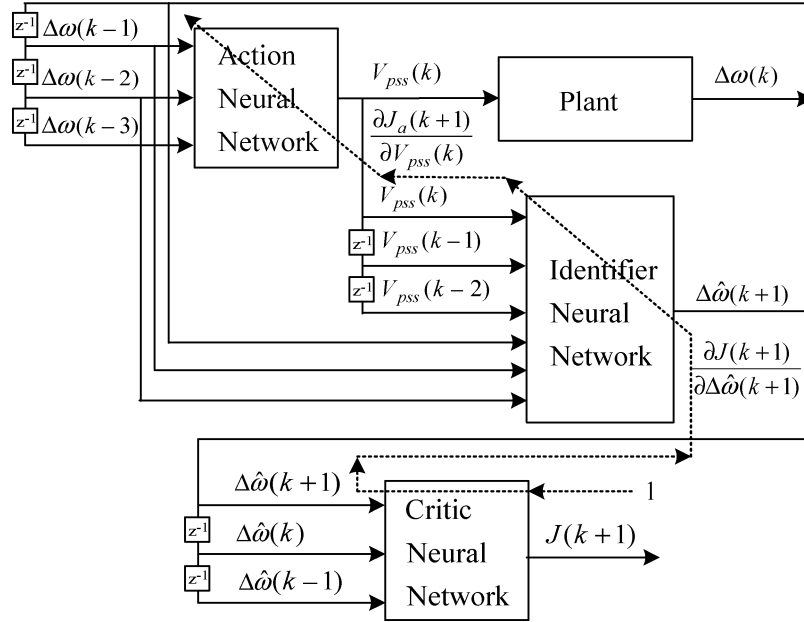
Fig. 8. Training process of the action network (dashed lines show first and second backpropagation pathways).

definition of $J(k)$, $J(k) = \gamma J(k+1) + U(k)$. Therefore, $\gamma J(k+1) + U(k)$ is the desired target output for $J(k)$ during the critic network training.

E. Action Neural Network Design

The action network is a multilayer feedforward network trained with the BP algorithm. The number of neurons in input, hidden and output layers is chosen empirically to be three, six, and one, respectively. The inputs to the action network is the actual speed deviation $\Delta\omega$ and its two previous values and its output is the supplementary control signal V_{pss}.

The training process of the action network is illustrated in Fig. 8. The purpose of action network training is to minimize the estimated *cost-to-go* function by the critic network with effective control signals. In HDP, $\partial J/\partial J$ is backpropagated through the critic and identifier networks in order to evaluate the performance of the action network and update its weights accordingly.

F. Training Procedure

The general training procedure and more details on ACD are described in [27]. It consists of three separate training cycles: training of the critic network, training of the identifier network and training of the action network. The training frequency for each training cycle may be different. To decrease the computation burden of the training process, training is carried once per sample and the learning rate is set to 0.1 with a sampling frequency of 20 Hz. The critic/action network training cycles are alternated until an acceptable plant performance is achieved.

IV. SIMULATION RESULTS

The training of the identifier and controller (corresponding to the action network in the HDP design) neural networks using the IDNC scheme is described in [21]. The critic neural network is trained based on the trained weights of the identifier and action neural network that give some stabilizing control at given operating point. During the training of the critic network,
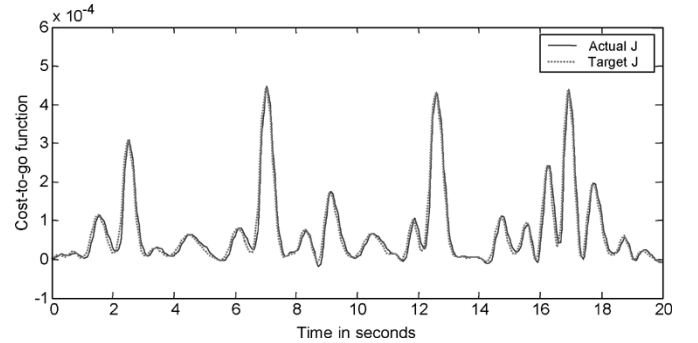

Fig. 9. Actual and expected cost-to-go function under forced training of the critic neural network ($\gamma = 0.5$, $P = 0.334$ pu, $Q = 0.001$ pu).

the weights of the identifier and action neural networks are kept fixed. The training of the critic network comprises two phases, which are forced training (with PRBS signal applied) and natural training [21]. To compare the impact of choice of γ values in the cost-to-go function on the controller performance, different γ values are selected and results are presented.

A. Training of the Critic Neural Network

1) Forced Training: During this phase, the V_{TREF} in Fig. 1 is replaced with a PRBS, which perturbs the plant around the stable value of V_{TREF} at a given operating point ($P = 0.334$ pu and $Q = 0.001$ pu). Fig. 9 shows the comparison of the actual and target cost-to-go function J, which are defined as $J(t)$ and $J_d(t)$, respectively. From Fig. 9 it can be seen that the training of the critic network has already converged.

2) Natural Training: During this phase, the critic network is trained under different kinds of small and large disturbances for the same plant operating point as in the forced training above. Fig. 10 shows the comparison of costs in response to a 200-ms three-phase short-circuit fault applied on the infinite bus for different γ values (0.2, 0.5, and 0.8).

To study the effect of different γ values on the control performance, the comparisons of control signal, speed deviation,
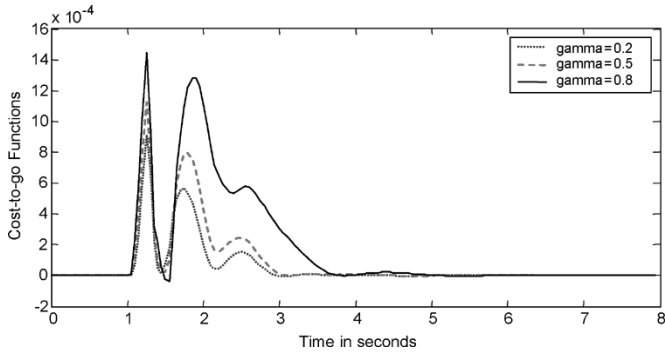
Fig. 10. Cost-to-go function for different γ response to a 200-ms three-phase short-circuit fault ($P = 0.334$ pu, $Q = 0.001$ pu).
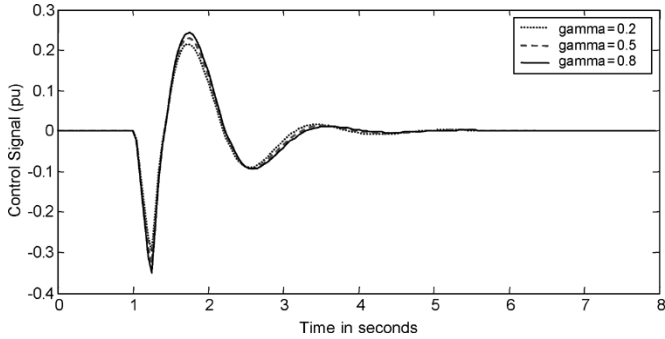

Fig. 11. Control signal response to the 200-ms three-phase short-circuit fault ($P = 0.334$ pu, $4Q = 0.001$ pu) with different discount factors in HDP critic training.
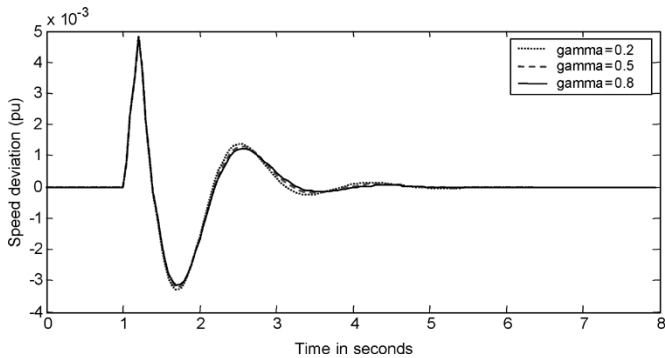

Fig. 12. Speed deviation response to a 200-ms three-phase short-circuit fault ($P = 0.334$ pu, $Q = 0.001$ pu) with different discount factors in HDP critic training.

and terminal voltage are provided in Figs. 11–13. From Figs. 12 and 13, it can be seen that the case of $\gamma = 0.8$ can give a little better performance for $\Delta\omega$ than the case of $\gamma = 0.5$, but it gives a little worse performance for V_t than the cases of $\gamma = 0.2$ and $\gamma = 0.5$. This is because $\Delta\omega$ is the control objective and defined in the utility function while V_t is not. When the discount factor γ is close to zero, the control objective emphasis on near-term stability and this strategy is close to the adaptive control based on next time-step error, while a discount factor close to unity emphasis on long-term stability, and the strategy is optimal control. Based on the controller performance achieved with different discount factor settings, γ is chosen to be 0.5 for the HDPC design.

B. Evaluation of HDPC PSS Performance

To evaluate the performance of the HDPC, the system response of the HDPC is compared with the cases where there
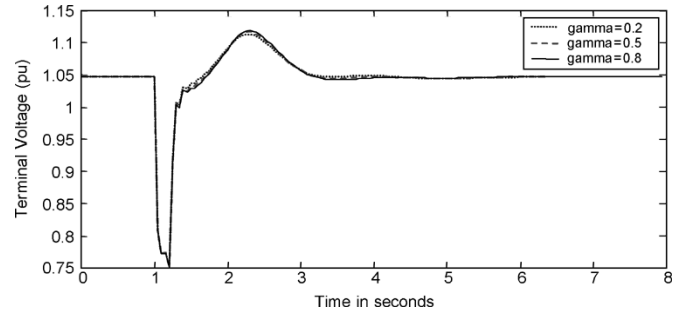

Fig. 13. Terminal voltage response to a 200-ms three-phase short-circuit fault ($P = 0.334$ pu, $Q = 0.001$ pu) with different discount factors in HDP critic training.
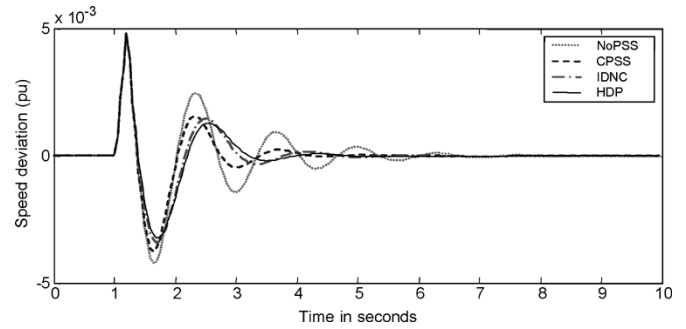

Fig. 14. Speed deviation response to a 200-ms three-phase short-circuit fault ($P = 0.334$ pu, $Q = 0.001$ pu).
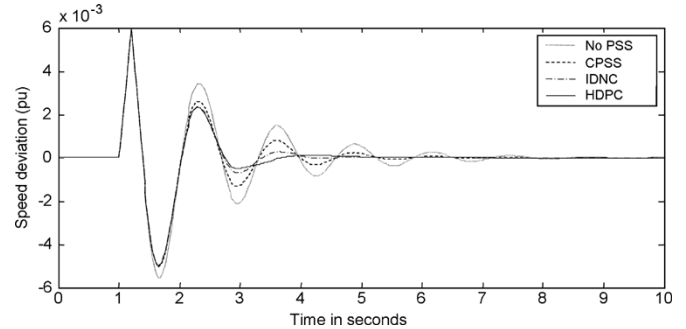

Fig. 15. Speed deviation response to a 200-ms three-phase short-circuit fault ($P = 0.5$ pu, $Q = 0.02$ pu).

is no PSS, with a CPSS, and with an indirect-adaptive-neuro-control-based PSS (IDNC) [21] in the system. The comparison is carried out under different kinds of operating conditions and disturbances. These disturbances are: a three-phase short circuit at the infinite bus, step changes in the terminal voltage reference, and change in transmission line impedance. All these disturbances are carried out under three different operating points, $P = 0.334$ pu, $Q = 0.001$ pu, $P = 0.5$ pu, $Q = 0.02$ pu, and $P = 0.6$ pu, $Q = 0.05$ pu.

1) First Operating Point: $P = 0.334$ pu, $Q = 0.001$ pu: Fig. 14 is the comparison of speed deviation response under a 200-ms three-phase short-circuit fault applied on the infinite bus at 1 s. It can be seen that HDP performance is comparable with that of CPSS. The parameters of the CPSS are fine tuned for this operating point and kept fixed for the following tests. It also can be seen that a fine-tuned CPSS can provide very good damping for its nominal operating point.

2) Second Operating Point: $P = 0.5$ pu, $Q = 0.02$ pu: Figs. 15 and 16 are the comparisons of the system responses
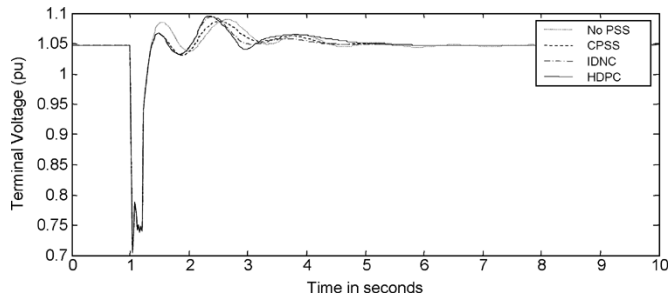
Fig. 16. Terminal voltage response to a 200-ms three-phase short-circuit fault ($P = 0.5$ pu, $Q = 0.02$ pu).
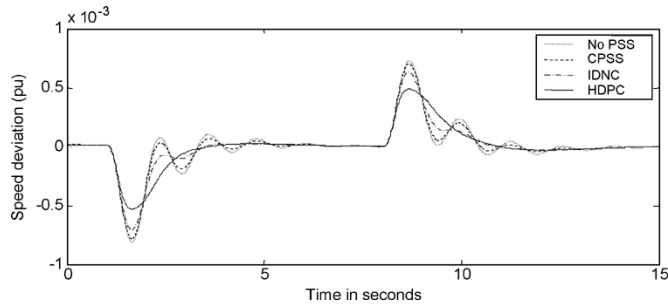

Fig. 17. Speed deviation response to 10% step changes in the reference of the terminal voltage ($P = 0.5$ pu, $Q = 0.02$ pu).

Fig. 18. Terminal voltage response to 10% step changes in the reference of the terminal voltage ($P = 0.5$ pu, $Q = 0.02$ pu).

Fig. 19. Speed deviation response for a change in transmission line impedance ($P = 0.5$ pu, $Q = 0.02$ pu).

Fig. 20. Speed deviation response to a 200-ms three-phase short-circuit fault ($P = 0.6$ pu, $Q = 0.05$ pu).
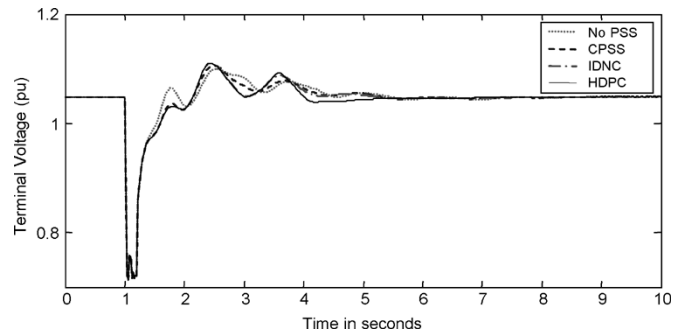
Fig. 21. Terminal voltage response to a 200-ms three-phase short-circuit fault ($P = 0.6$ pu, $Q = 0.05$ pu).

Fig. 22. Speed deviation response to 10% step changes in the reference of the terminal voltage ($P = 0.6$ pu, $Q = 0.05$ pu).
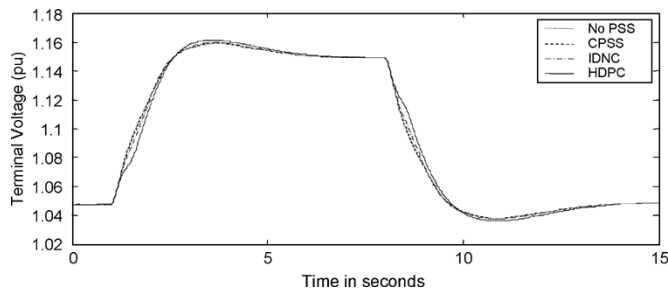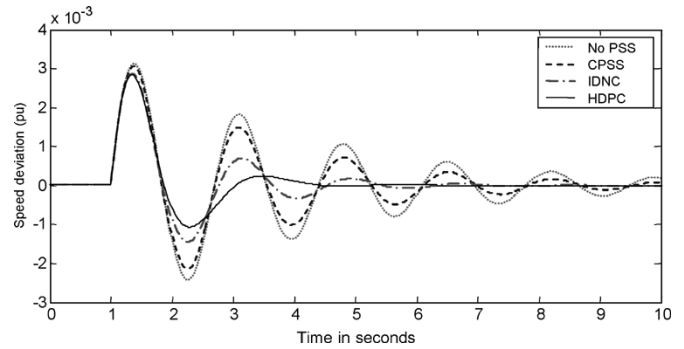
under a 200-ms three-phase short-circuit fault applied on the infinite bus at 1 s. It can be seen that CPSS has better damping for the speed deviation than when there is no CPSS in the system; IDNC has better damping than CPSS while HDPC has the best damping. From Fig. 16, it can be seen that the terminal voltage responses are comparable for this particular fault.

Figs. 17 and 18 are the comparisons of the system response to a 10% step change in V_{TREF} (1.1–1.21 pu) at 1 second and 10% decrease (1.21–1.1 pu) at 8 s. Again, the HDPC provides the best damping for the speed deviation for this kind of disturbance and the terminal voltage responses are similar.

Fig. 19 is the comparison of the system responses to a change in transmission line impedance. During this case, the impedance of the transmission line is changed from $Z_1 = 0.025 + j0.7559$ pu to $Z_2 = 0.05 + j1.5$ pu at 1 s. Again, the HDP provides the best damping for the speed deviation of the four controllers. The responses of the terminal voltage of the different controllers are comparable.

3) Third Operating Point:: $P = 0.6$ pu, $Q = 0.05$ pu

Figs. 20 and 21 are comparisons of the system responses under a 200-ms three-phase short-circuit fault applied at the infinite bus at 1 s. The findings of the simulation results are similar to the conclusions for the first operating point above.

Figs. 22 and 23 are the comparison of the system response to 10% step change in V_{TREF}, that is, 10% increase from $V_{\text{TREF}} =$

Fig. 23.   Terminal voltage response to 10% step changes in the reference of the terminal voltage ($P = 0.6$ pu, $Q = 0.05$ pu).

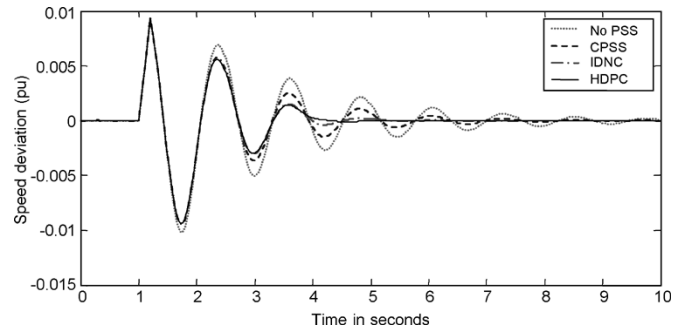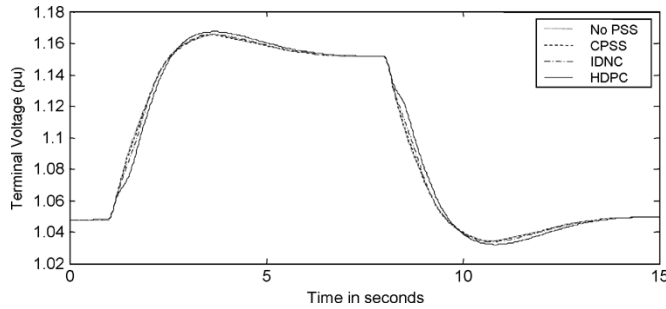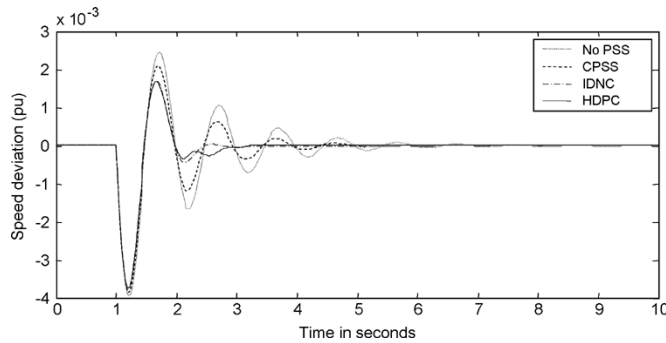Fig. 24.   Speed deviation response for a change in transmission line impedance ($P = 0.6$ pu, $Q = 0.05$ pu).

1.1 pu to $V_{\text{TREF}} = 1.21$ pu at 1 s and 10% decrease from $V_{\text{TREF}} = 1.21$ pu to $V_{\text{TREF}} = 1.1$ pu at 8 s. Again, the conclusions are similar to those for the first operating point above.

Fig. 24 is the comparison of the system responses to a simulated transmission line fault. The impedance of the transmission line changes from $Z_1 = 0.025 + j0.7559$ pu to $Z_2 = 0.0125 + j0.378$ pu at 1 s. For this test, the HDPC still has the best damping performance.

V. Conclusion

To overcome the drawbacks of CPSSs, an HDP-based PSS design has been presented in this paper. The proposed method was evaluated on an SMIB. The design of the HDP is based on only the speed deviation signals of the synchronous generator. Therefore, the computations involved in the proposed PSS design are minimal. This is desirable for practical hardware implementation on the power station platforms. In addition, the online training computational demand is reduced, once the action network is trained for optimal performance, over a number of operating points. Simulation results, for different kinds of small and large disturbances, under different operating conditions, demonstrate the effectiveness and robustness of the HDP-based PSS.

Such a nonlinear adaptive/robust PSS design based on ACD yields better and fast damping under small and large disturbances, especially with changes in system operating conditions. Better and fast damping means that generators can operate closer to their maximum generation capacity. This ensures that generators remain stable under severe faults such as three-phase short circuits.

TABLE I.
PARAMETERS OF THE SINGLE MACHINE INFINITE BUS POWER SYSTEM IN FIG. 1

$T_{d0}'=6.69s$	$T_{q0}''=0.25s$	$X_d'=0.205pu$	$T_d'=0.66s$
$T_q''=27ms$	$X_d''=0.164pu$	$T_{d0}''=33ms$	$T_{kd}=38ms$
$X_q=1.98pu$	$T_d''=26.4ms$	$X_d=2.09pu$	$X_q''=0.213pu$
$T_{T1}=0.15$	$T_{T2}=0.594$	$T_{T3}=0.884$	$T_{T4}=2.662$
$T_{MMIN}=0$	$T_{MMAX}=1.2$	$K_G=20$	$T_{G1}=0.264$
$T_{G2}=0.0264$	$K_A=50$	$T_A=0.01$	$V_{AMIN}=-10$
$V_{AMAX}=10$	$T_E=0.46$	$V_{FMIN}=0.5$	$V_{FMAX}=3$
$K_F=0.1$	$T_F=1$	$K_{STAB}=25$	$T_W=10$
$T_1=0.76$	$T_2=0.1$	$T_3=0.76$	$T_4=0.1$
$V_{PSS\_MIN}=-0.1$	$V_{PSS\_MAX}=0.1$		

Appendix

See Table I.

References

[1] E. V. Larsen and D. A. Swann, "Applying power system stabilizers, part I, II, III," *IEEE Trans. Power App. Syst.*, vol. PAS-100, no. 6, pp. 3017–3041, Nov./Dec. 1981.

[2] M. A. Abido, "Robust design of multimachine power system stabilizers using simulated annealing," *IEEE Trans. Energy Convers.*, vol. 15, no. 3, pp. 297–304, Sep. 2000.

[3] Y. L. Abdel-Magid, M. A. Abido, and A. H. Mantaway, "Robust tuning of power system stabilizers in multi-machine power systems," *IEEE Trans. Power Syst.*, vol. 15, no. 2, pp. 735–740, May 2000.

[4] A. L. B. Do Bomfim, G. N. Taranto, and D. M. Falcao, "Simultaneous tuning of power system damping controllers using genetic algorithms," *IEEE Trans. Power Syst.*, vol. 15, no. 1, pp. 163–169, Feb. 2000.

[5] K. A. El-Metwally, G. C. Hancock, and O. P. Malik, "Implementation of a fuzzy logic PSS using a micro-controller and experimental test results," *IEEE Trans. Energy Convers.*, vol. 11, no. 1, pp. 91–96, Mar. 1996.

[6] A. Hariri and O. P. Malik, "A fuzzy logic based power system stabilizer with learning ability," *IEEE Trans. Energy Convers.*, vol. 11, no. 4, pp. 721–727, Dec. 1996.

[7] J. W. Chapman, M. D. Ilic, C. A. King, L. Eng, and H. Kaufman, "Stabilizing a multi-machine power system via decentralized feedback linearizing excitation control," *IEEE Trans. Power Syst.*, vol. 8, no. 3, pp. 830–839, Aug. 1993.

[8] M. Nambu and Y. Ohsawa, "Development of an advanced power system stabilizer using a strict linearization approach," *IEEE Trans. Power Syst.*, vol. 11, no. 2, pp. 813–818, May 1996.

[9] A. Soos and O. P. Malik, "An H_2 optimal adaptive power system stabilizer," *IEEE Trans. Energy Convers.*, vol. 17, no. 1, pp. 143–149, Mar. 2002.

[10] T. Hiyama and K. Tomsovic, "Current status of fuzzy system applications in power systems," in *Proc. IEEE SMC'99*, Tokyo, Japan, 1999, pp. 527–532.

[11] Y. Y. Hsu and C. L. Chen, "Tuning of power system stabilizers using an artificial neural network," *IEEE Trans. Energy Convers.*, vol. 6, no. 4, pp. 612–619, Dec. 1991.

[12] R. Segal, M. L. Kothari, and S. Madnani, "Radial basis function (RBF) network adaptive power system stabilizer," *IEEE Trans. Power Syst.*, vol. 15, no. 2, pp. 722–727, May 2000.

[13] Y. M. Park, S. H. Hyun, and J. H. Lee, "A synchronous generator stabilizer design using neuro inverse controller and error reduction network," *IEEE Trans. Power Syst.*, vol. 11, no. 4, pp. 1969–1975, Nov. 1996.

[14] Y. Zhang, O. P. Malik, G. S. Hope, and G. P. Chen, "Application of an inverse input/output mapped ANN as a power system stabilizer," *IEEE Trans. Energy Convers.*, vol. 9, no. 3, pp. 433–441, Sep. 1994.

[15] P. Shamsollahi and O. P. Malik, "Direct neural adaptive control applied to synchronous generator," *IEEE Trans. Energy Convers.*, vol. 14, no. 4, pp. 1341–1346, Dec. 1999.

[16] B. Changaroon, S. C. Srivastava, and D. Thukaram, "A neural network based power system stabilizer suitable for on-line training-a practical case study for EGAT system," *IEEE Trans. Energy Convers.*, vol. 15, no. 1, pp. 103–109, Mar. 2000.

[17] J. He and O. P. Malik, "An adaptive power system stabilizer based on recurrent neural networks," *IEEE Trans. Energy Convers.*, vol. 12, no. 4, pp. 413–418, Dec. 1997.

[18] T. Kobayashi and A. Yokoyama, "An adaptive neuro-control system of synchronous generator for power system stabilization," *IEEE Trans. Energy Convers.*, vol. 11, no. 3, pp. 621–630, Sep. 1996.

[19] P. Shamsollahi and O. P. Malik, "An adaptive power system stabilizer using on-line trained neural networks," *IEEE Trans. Energy Convers.*, vol. 12, no. 4, pp. 382–387, Dec. 1997.

[20] Y. M. Park, M. S. Choi, and K. Y. Lee, "A neural network-based power system stabilizer using power flow characteristics," *IEEE Trans. Energy Convers.*, vol. 11, no. 2, pp. 435–441, Jun. 1996.

[21] W. Liu, G. K. Venayagamoorthy, and D. C. Wunsch, "Design of an adaptive neural network based power system stabilizer," *Neural Netw.*, vol. 16, no. 5–6, pp. 891–898, 2003.

[22] G. Sybille, P. Brunelle, R. Champagne, L. Dessaint, and H. Lehuy, *Power System Blockset, version 2.0.* Natick, MA: The MathWorks Inc., 2000.

[23] P. Kundur, M. Klein, G. J. Rogers, and M. S. Zywno, "Application of power system stabilizers for enhancement of overall system stability," *IEEE Trans. Power Syst.*, vol. 4, no. 2, pp. 614–626, May 1989.

[24] *IEEE Recommended Practice for Excitation System Models for Power System Stability Studies*, IEEE Std. 421.5-1992.

[25] G. K. Venayagamoorthy and R. G. Harley, "A continually online trained neurocontroller for excitation and turbine control of a turbogenerator," *IEEE Trans. Energy Convers.*, vol. 16, no. 3, pp. 261–269, Sep. 2001.

[26] P. J. Werbos, "Approximate dynamic programming for real-time control and neural modeling," in *Handbook of Intelligent Control*, D. A. White and D. A. Sofge, Eds. New York: Van Nostrand Reinhold, 1992, pp. 493–525.

[27] G. K. Venayagamoorthy, R. G. Harley, and D. C. Wunsch, "Comparison of heuristic dynamic programming and dual heuristic programming adaptive critics for neurocontrol of a turbogenerator," *IEEE Trans. Neural Netw.*, vol. 13, no. 3, pp. 764–773, May 2002.

[28] D. Prokhorov and D. C. Wunsch, "Adaptive critic designs," *IEEE Trans. Neural Netw.*, vol. 8, no. 6, pp. 997–1007, Nov. 1997.

[29] K. S. Narendra and K. Parthasarathy, "Identification and control of dynamical systems using neural networks," *IEEE Trans. Neural Netw.*, vol. 1, no. 1, pp. 4–27, Mar. 1990.

Ganesh Kumar Venayagamoorthy (M'97–SM'02) received the B.Eng. (Honors) degree with first class honors in electrical and electronics engineering from Abubakar Tafawa Balewa University, Bauchi, Nigeria, in 1994, and the M.Sc.Eng. and Ph.D. degrees in electrical engineering from the University of Natal, Durban, South Africa, in 1999 and 2002, respectively.

He was a Senior Lecturer at the Durban Institute of Technology, South Africa, prior to joining the University of Missouri, Rolla (UMR), as an Assistant Professor in the Department of Electrical and Computer Engineering in May 2002. He directs the Real-Time Power and Intelligent Systems (RTPIS) Laboratory at UMR. His research interests are in computational intelligence, power systems, evolvable hardware, and signal processing. He has authored over 130 publications, and has attracted over $1 million in research funding.

Dr. Venayagamoorthy is the 2005 IEEE Industry Application Society (IAS) Outstanding Young Member award recipient, a 2004 NSF CAREER award recipient, the 2004 IEEE St. Louis Section Outstanding Young Engineer, the 2003 International Neural Network Society (INNS) Young Investigator award recipient, a 2001 recipient of the IEEE Computational Intelligence Society (CIS) W. J. Karplus summer research grant and the recipient of five prize papers with the IEEE IAS and IEEE CIS. He is an Associate Editor of the IEEE TRANSACTIONS ON NEURAL NETWORKS. He is a Senior Member of the South African Institute of Electrical Engineers and a Member of INNS and the American Society for Engineering Education. He is currently the IEEE St. Louis CIS and IAS Chapter Chairs, the Chair of the Task Force on Intelligent Control Systems, and the Secretary of the Intelligent Systems Subcommittee of the IEEE Power Engineering Society. He was the Technical Program Co-Chair of the 2003 International Joint Conference on Neural Networks, Portland, OR, and of the 2004 International Conference on Intelligent Sensing and Information Processing, Chennai, India.
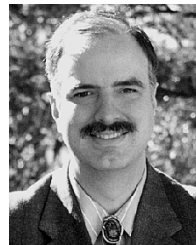
Donald C. Wunsch, II (S'87–M'92–SM'94–F'05) received the B.S. degree in applied mathematics from the University of New Mexico, Albuquerque, and the M.S. degree in applied mathematics and the Ph.D. degree in electrical engineering from the University of Washington, Seattle.

He is the Mary K. Finley Missouri Distinguished Professor of Computer Engineering at the University of Missouri, Rolla, where he has been since 1999. His prior positions were Associate Professor and Director of the Applied Computational Intelligence Laboratory at Texas Tech University, Senior Principal Scientist at Boeing, Consultant for Rockwell International, and Technician for International Laser Systems. He has authored over 200 publications, and has attracted over $5 million in research funding. He has been the advisor to eight Ph.D. students—four in electrical engineering, three in computer engineering, and one in computer science.

Prof. Wunsch has been the recipient of many awards, including the Halliburton Award for Excellence in Teaching and Research and the National Science Foundation CAREER Award. He served as a voting member of the IEEE Neural Networks Council, Technical Program Co-Chair for IJCNN'02, General Chair for IJCNN'03, International Neural Networks Society Board of Governors Member, and is currently President of the International Neural Networks Society.

Wenxin Liu (S'01) received the B. Eng. degree in industrial automation and the M. Eng. degree in control theory and control engineering from Northeastern University, Shenyang, China, in 1996 and 2000, respectively, and the Ph.D. degree in electrical engineering from the University of Missouri, Rolla (UMR), in 2005.

He is currently a Postdoctoral Fellow with the Center for Advanced Power Systems, Florida State University, Tallahassee. His current research interests include nonlinear control, neural network control, power systems, and system engineering.